

Unraveling the connection between high-order magnetic interactions and local-to-global spin Hamiltonian in non-collinear magnetic dimers

Ramon Cardias,^{1,2} Jhonatan dos Santos Silva,^{3,4} Anders Bergman,⁵ Attila Szilva,⁵ Yaroslav O. Kvashnin,⁵ Jonas Fransson,⁵ Angela B. Klautau,^{3,6} Olle Eriksson,⁵ Anna Delin,^{1,7} and Lars Nordström⁵

¹*Department of Applied Physics, School of Engineering Sciences,*

KTH Royal Institute of Technology, AlbaNova University Center, SE-10691 Stockholm, Sweden

²*Instituto de Física, Universidade Federal Fluminense, 24210-346, Niterói RJ, Brazil*

³*Faculdade de Física, Universidade Federal do Pará, Belém, PA, Brazil*

⁴*Instituto Federal de Educação, Ciência e Tecnologia do Pará, Óbidos, PA, Brazil*

⁵*Department of Physics and Astronomy, Uppsala University, 75120 Box 516 Sweden*

⁶*Departamento de Física da Universidade de Aveiro, 3810-183 Aveiro, Portugal*

⁷*Swedish e-Science Research Center (SeRC), KTH Royal Institute of Technology, SE-10044 Stockholm, Sweden*

(Dated: June 13, 2023)

A spin Hamiltonian, which characterizes interatomic interactions between spin moments, is highly valuable in predicting and comprehending the magnetic properties of materials. A deeper understanding of the microscopic origin of magnetic interactions can open new pathways toward realizing nanometer-scale systems for future spintronic devices. Here, we explore a method for explicitly calculating interatomic exchange interactions in non-collinear configurations of magnetic materials considering only a bilinear spin Hamiltonian in a local scenario. Based on density-functional theory (DFT) calculations of dimers adsorbed on metallic surfaces, and with a focus on the Dzyaloshinskii-Moriya interaction (DMI) which is essential for stabilizing chiral non-collinear magnetic states, we discuss the interpretation of the DMI when decomposed into microscopic electron and spin densities and currents. We clarify the distinct origins of spin currents induced in the system and their connection to the DMI. In addition, we reveal how non-collinearity affects the usual DMI, which is solely induced by spin-orbit coupling, and DMI-like interactions brought about by non-collinearity. We explain how the dependence of the DMI on the magnetic configuration establishes a connection between high-order magnetic interactions, enabling the transition from a local to a global spin Hamiltonian.

I. INTRODUCTION

In order to calculate the magnetic properties of a given system, one of the most used solutions is to start from a spin Hamiltonian that describes the interatomic interactions between the atomic spins by assuming that it is possible to identify well-defined regions of a material where the magnetisation density is more or less unidirectional and sizeable only close to an atomic nucleus. One of the best example for a spin Hamiltonian is the generalized bilinear classical spin model which is written as

$$\mathcal{H} = - \sum_{\langle ij \rangle} \left(J_{ij} \vec{e}_i \cdot \vec{e}_j + \vec{D}_{ij} \cdot (\vec{e}_i \times \vec{e}_j) + \vec{e}_i \cdot \mathcal{A}_{ij} \cdot \vec{e}_j \right), \quad (1.1)$$

where J_{ij} is the scalar Heisenberg exchange coupling parameter, \vec{D}_{ij} is the Dzyaloshinskii-Moriya interaction (DMI) vector, \mathcal{A}_{ij} is the symmetric anisotropic interaction term, \vec{e}_i and \vec{e}_j are unit vectors describing the direction of the magnetic moment of the atom as site i and j , respectively, and the summation is made over pairs of atoms $\langle ij \rangle$. The definition of Eq. 1.1 is the same as defined in Ref. [1]. Many methods have been proposed in the recent literature regarding how to calculate these parameters [1–5]. One that has been widely used is the one proposed in Refs. [1, 6] and we will refer to it as the Liechtenstein-Katsnelson-Antropov-Gubanov (LKAG) method. It is based on the magnetic force theorem [7, 8], which assumes that an effective spin Hamiltonian accurately describes the energy of different atomic spin configurations, that are close to the magnetic ground state. In other words, the electronic Kohn-Sham Hamiltonian can be mapped onto

a (classical) spin Hamiltonian since the variation of total energy of the electronic sub-system can be expressed in terms of variations only of occupied single particle states.

It is known that in all LKAG-like approaches, especially when the magnetic state is allowed to have any non-collinear order [9], the interatomic exchange coupling parameters depend on the underlying spin configuration, i.e., the mapped spin model is only valid in a local region of the energy vs. configuration curve, i.e., it is only relevant for small magnetic variations around the reference state. This is in contrast to the concept of global spin models, in which high-order terms are required to correctly describe the energy landscape for many magnetic configurations, not just around a chosen point in configuration space, but globally. In practice, this means that the electron hops not only between the two crystal atomic sites considered, but also between other sites and one can think of these high-order terms as multi-spin interactions [10–13]. The problem arises when it becomes very difficult to reach completeness, i.e. how many multi-spin interactions should be considered, and the configuration space is too large to get a hold of a proper physical conclusion. Even in a simple system, such as an Fe dimer, with a non-collinear magnetic configuration, the Heisenberg picture is broken [14]. In fact, these two approaches are complementary, since if the state dependence is taken into account for a local spin model in an LKAG-like approach, all global symmetries should be recovered. However, the actual link between the magnetic configuration-dependent and the multi-spin representations is often unclear. In this work, we show the connection between the magnetic configuration-dependent and multi-spin repre-

sentations in case of dimers, by explicitly showing how the non-collinearity-induced DMI-like and the relativistic DMI behave, while providing insight into their microscopic origins.

More specifically, we have developed a technique to calculate the interactions described in Eq. 1.1 for any magnetic configuration considering only a bilinear spin Hamiltonian [15, 16]. The dependence of these parameters on the magnetic configuration has been revealed, which can be interpreted as the emergence of high-order terms folded onto a bilinear Hamiltonian expression as the non-collinear magnetic texture arises. In this way, one does not have access on the multi-spin perspective of the problem, but on the other hand, one can consider a simple solution to study the magnetic properties locally in configuration space. This approach (technique), combined with atomistic spin dynamics, has been shown to significantly refine the comparison between theory and experiment when considering properties of excited states, such as the magnon softening induced by temperature effects, as demonstrated in Refs. 9 and 17. Moreover, in Refs. 16 and 15 we have shown that these interactions can be seen in terms of spin/charge density and spin/charge currents. The results presented in the latter references have shown that the DMI calculated from a non-collinear magnetic configuration have strong magnitude and, most importantly, have a non-chiral behaviour, which goes against the original works of Moryia and Dzyaloshinskii [18, 19]. That issue was addressed in previous works by naming this extra behaviour as a DMI-like term, suggesting that in the presence of a non-collinear magnetic texture, both usual DMI and DMI-like interactions should co-exist. In Refs. 15 and 16, as well as in the work by Dos Santos and collaborators [20], it was proposed that the non-relativistic DMI-like interaction arises from high-order terms, or multi-spin interactions. It was also argued that a set of configuration independent magnetic interaction parameters should suffice to describe the system if the proper spin Hamiltonian is used. Moreover, the extensive discussion about spin Hamiltonian and how to correctly map onto an electronic Hamiltonian can be seen in Ref. [1] and the references therein.

This paper has the following structure: In Sec. II, we discuss about the structure of the DMI calculated via first principle and its dependence on spin- and charge-currents. Our results Section is split in 3 subsections, where in Sec.III.A, we explain the different origins of spin-currents induced into the system and how they relate with the DMI, in Sec.III.B we used the real space - muffin-tin orbitals - atomic sphere approximation (RS-LMTO-ASA) method [21–25] to calculate the DMI between the two magnetic moments of a dimer of Cr, Mn and Fe on top of W(001), Pt(001) and Cu(001) surfaces, for a set of different magnetic configurations where we unveil how the non-collinearity affects the DMI (solely induced by SOC) and the DMI-like (induced non-collinearity), and lastly in Sec.III.C we explain how the magnetic dependence of the DMI connects with the high-order magnetic interactions and creating a bridge between a local to a global spin Hamiltonian.

II. METHOD

The Kohn-Sham equation, which has the form of a single particle Schrödinger equation, can be written as

$$\begin{aligned} i\frac{\partial\psi}{\partial t} &= H\psi \\ H &= -\nabla^2 + V(\mathbf{r}) - \left(\vec{B}_{xc}(\mathbf{r}) + \vec{B}_{ext}(\mathbf{r})\right) \cdot \vec{\sigma} \end{aligned} \quad (2.1)$$

where $V(\mathbf{r})$ is the effective potential, $\vec{B}_{ext}(\mathbf{r})$ and $\vec{B}_{xc}(\mathbf{r})$ are the external magnetic field and the exchange-correlation field, respectively, that couple to the electrons spin, and $\vec{\sigma}$ stands for the Pauli spin matrices $\{\sigma_x, \sigma_y, \sigma_z\}$. Note that Rydberg units are used here: $\hbar = 2m = e^2/2 = 1$. It is noteworthy that on Appendix A, we use a different definition of the wave function, using capital Ψ . From the Kohn-Sham Hamiltonian one can calculate the Green function as

$$G(z) = (z - H)^{-1}, \quad (2.2)$$

where $z \in \mathbb{C}$. Note that $G(z)$ can be decomposed into inter-site terms, G_{ij} , since $G(z) = \sum_{ij} |\phi_i\rangle G_{ij} \langle \phi_j|$ with local functions $|\phi_i\rangle$ at site i , which can be further decomposed into spin-components as

$$G_{ij} = G_{ij}^0 + \vec{G}_{ij} \cdot \vec{\sigma}, \quad (2.3)$$

where \vec{G}_{ij} is a vector with the components of G_{ij}^x , G_{ij}^y and G_{ij}^z . We introduce here the notation G_{ij}^η , where the index η enumerates both the scalar spin-independent Green function as well as the components of the spin-dependent vector Green function of Eq. (2.3), i.e. η can be either 0, x , y or z . We will refer here to G_{ij}^0 as the charge part and to \vec{G}_{ij} as the spin part of the Green function. Note that one can further decompose the components of the Green function into terms that are either even or odd under time reversal symmetry [26]. This can be done by introducing $G_{ij}^{\eta\kappa}$ where the first index η has been introduced and explained after Eq. (2.3) while the second index κ can be viewed as an indicator whether the terms that are time reversal invariant and those are not, i.e. κ can be 0 or 1 (the exact relation is explained below). This decomposition of the Green function can be summarised as,

$$G_{ij}^\eta = G_{ij}^{\eta 0} + G_{ij}^{\eta 1}, \quad (2.4)$$

where G_{ij}^{00} and \vec{G}_{ij}^1 are time reversal invariant while G_{ij}^{01} and \vec{G}_{ij}^0 are not. Sometimes it is convenient to write the x , y or z dependent components of the Green function as vectors, i.e. \vec{G}_{ij}^κ . This decomposition also plays a useful role in how the Green function behave under site exchange, since in a real local basis [26] we have that

$$G_{ij}^{\eta\kappa} = (-1)^\kappa G_{ji}^{\eta\kappa T}. \quad (2.5)$$

In fact, it has been shown that these two index Green functions are decomposed in terms that produce local charge-, G^{00}

or spin-densities, \vec{G}^0 , and charge-, G^{01} , and spin-currents \vec{G}^1 , respectively [1]. Once the the Green function is given, the (integrated) density of states and the grand canonical potential (Ω) of the electronic sub-system can also be determined.

As a next step, and as reviewed in Ref.[1], one can introduce a small variation of the atomic spin at site i and derive the variation of the grand potential compared to a reference state (the ground state). The same procedure can be done at the level of a spin Hamiltonian and then the variation of the spin Hamiltonian, $\delta\mathcal{H}$, can be compared with the variation of the grand canonical potential, $\delta\Omega$. One can make small rotations at the spin at site i and j and the same time and the fact that the rotations are made simultaneously leads to the the emergence of an extra, interacting, term at both levels. With the sign convention of Eq. 1.1, we get for the DMI term (obtained due to two site rotations) that

$$D_{ij}^{(2)\nu} = \frac{4}{\pi} \Re \int \text{Tr}_L (B_i G_{ij}^{00} B_j G_{ji}^{\nu 1} + B_i G_{ij}^{01} B_j G_{ji}^{\nu 0}) d\varepsilon, \quad (2.6)$$

where $D_{ij}^{(2)\nu}$ is a component of \vec{D}_{ij} and ν can x , y and z . Note that the details of the derivation and the explicit expression for the Heisenberg J_{ij} and the symmetric anisotropic interaction \mathcal{A}_{ij} can be found in Ref. 1.

III. RESULTS

A. Collinear vs noncollinear currents

It is known that the DMI emerges due to an intrinsic spin-current induced by the SOC [27]. This can be seen explicitly in Eq. 2.6, since the spin-current part of the Green function appears explicitly. In this formalism, the DMI was split in two different contributions, namely $D^S \propto G_{ij}^{\nu 1}$ and $D^C \propto G_{ij}^{01}$, spin- and charge-current induced, respectively. In the simple case of a dimer, D^C gives a weak contribution to the total DMI due to the fact that the magnetic configuration will always be co-planar. Apart from the spin-current induced by the SOC, the non-collinearity of the magnetic moments also induces a spin-current, but via a different mechanism. This is explored in more detail in Appendix A, in Eq. A15 where we obtain that

$$\vec{j}_s \propto (\vec{s}_1 \times \vec{s}_2). \quad (3.1)$$

This spin-current induced by the non-collinearity adds an extra term in the DMI and as a result the DMI will have two different contributions. For instance, we considered two rotations in different planes, as shown in Fig. 1: (top) in the xz plane and in (bottom) yz plane. In the (001) surface, if the bond between the two atoms is the x -axis, a DMI is found in the y -direction D_y according to Moryia rules [28]. If the rotation described in a) is performed, a spin current in the y -direction emerges and then one can see total DMI with both contributions, the SOC and the non-collinear, being in the y -direction. If rotation b) is done instead, the spin-current induced by the non-collinearity, according to Eq. 3.1, is in the

x -direction and then one can see two independent contributions that are not parallel. For the rotation of the spin moments specified in case (b), one can analyse the contributions separately.

In Appendix B we derive the reference dependence of both the two independent types of Dzyaloshinskii-Moriya like interactions, that differ in the origin of the spin currents, i.e., either non-collinearity or spin orbit coupling.

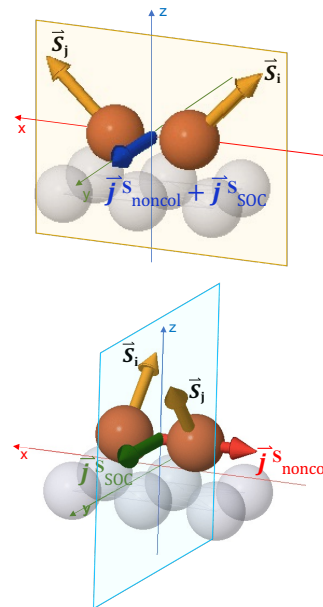


FIG. 1. Illustration of the spin-currents in a magnetic dimer. The dimer bond axis is along the x -direction, and the z -axis the surface normal. The atoms' spin magnetic moments (S_i, S_j) are represented by arrows. On top, the plane (xz) containing the non-collinear magnetic structure is parallel to the bond, and on bottom the magnetic moments are rotating in the yz plane, perpendicular to the bond. \vec{j}_{noncol} and \vec{j}_{SOC} denote the spin-currents induced by the non-collinearity of the magnetic moments and the SOC, respectively.

B. Dzyaloshinskii-Moriya interactions of dimers on various surfaces

In order to evaluate (quantify) these different contributions to the DMI, we present a systematic study of magnetic dimers on several non-magnetic surfaces. To be specific, we performed density functional theory (DFT) calculations, using the RS-LMTO-ASA method (see Computational details in Appendix C), for Cr, Mn and Fe dimers on surfaces where spin-orbit effects are expected to be significant (Pt(001) and W(001)) or weak (e.g. Cu(001)). To understand the dependence of the DMI with respect to the angle between the spin moments of the dimer atoms, (θ), and with respect to the SOC, we performed calculations of the DMI considering the rotational plane shown in Fig. 1(b), where the different contributions to the DMI are perpendicular and can be studied separately. We consider one magnetic moment fixed along the

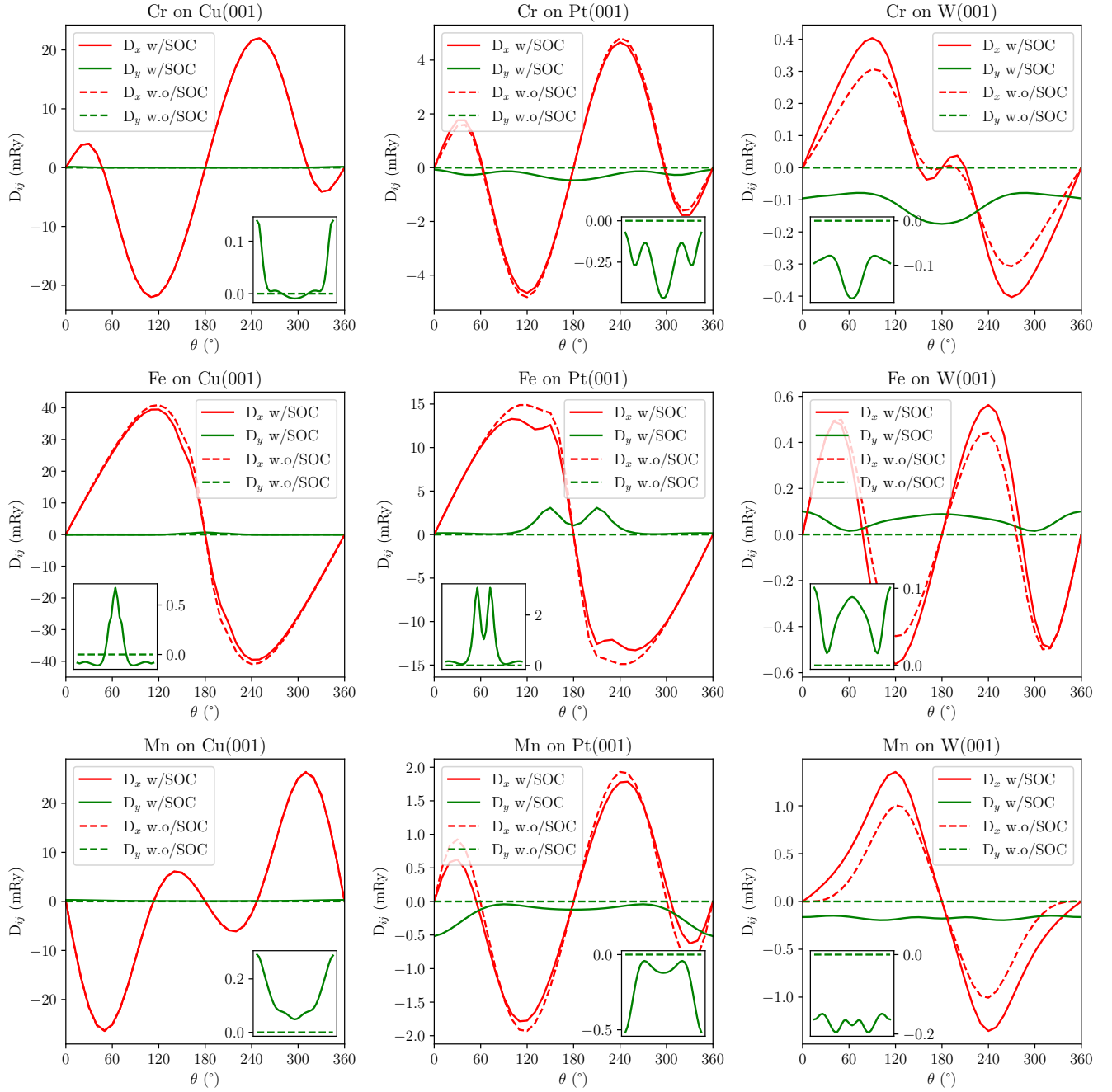


FIG. 2. DMI calculated when varying the vertical angle (θ) between the magnetic moments of the dimer atoms around the dimer bond axis (x-direction). The top panels display the results for Cr dimers on Cu(001), Pt(001), and W(001) from left to right, while the middle panels refer to the Fe dimers. The bottom panels refer to the Mn dimers on the same substrates. In each panel, the red lines denote the DMI component in the bonding direction of the atoms, D_x , while the green lines denote the DMI component perpendicular to the bond, D_y . The full lines stand for calculations when the spin-orbit coupling is included, whereas the dashed lines denote calculation without spin-orbit coupling (SOC). The insets represent a zoom into the D_y component. Here, we can see that the SOC-induced DMI is null if SOC is absent.

z-axis while the other one rotates around the x-axis with an angle θ . In that case, the non-collinearity will induce a spin-current in the x-axis giving rise to what we have termed the non-collinear DMI[15, 16], whereas SOC will induce a spin-

current parallel to the mirror plane between the atoms giving a finite DMI along the y-axis. One can see that in the case of the absence of SOC (dashed line), the SOC DMI (D_y) is immediately zero, while the non-collinear DMI (D_x) is still

finite. It is possible to see in Fig. 2 that the D_y has a chiral behaviour, i.e. $D_y(\theta) = D_y(-\theta)$, while the non-collinear DMI D_x does not, i.e. $D_x(\theta) = -D_x(-\theta)$. It means, in this particular setup, that the D_y is the one responsible to lift the degeneracy between two different rotational senses. These properties match the comment made by Manuel dos Santos Dias *et al.* in Ref. 20. It is important to point out that both SOC-DMI (D_y) and non-collinear DMI (D_x) are configuration dependent, but only D_y is fully dependent on SOC. The substrates Cu, W and Pt have an ascendant strength of SOC, which in this case translates to a direct proportional relation between SOC and the strength of the SOC induced DMI D_y . On the other hand, the non-collinear DMI-like D_x is seen to have an inversely proportional relationship with the SOC, being the weakest for the dimers on W(001). The dimers have a canted magnetic configuration as a ground state, either close to AFM or FM, as shown in Table I. For the dimers of Cr and Fe on Pt(001), our results are in good agreement with Ref. 29 with respect to the calculated magnetic interactions J_{12} and \vec{D}_{12} , although their predicted angles are slightly higher than our self-consistent calculations. Note that the amplitude of θ_{12} is proportional to $\frac{|\vec{D}_{12}|}{J_{12}}$, which is the highest in the case of Fe on W(001). Note that since the magnetic interactions are obtained from the magnetic ground-state, which is non-collinear, the vector DMI do not lie exclusively on the y-axis, but on the xy-plane.

	J_{12}	D_{12}	θ_{12} (°)
Cr ₂ /Cu(001)	-26.56	0.03	180
Mn ₂ /Cu(001)	-3.20	1.72	174
Fe ₂ /Cu(001)	9.56	0.50	1
Cr ₂ /W(001)	0.88	0.13	5
Mn ₂ /W(001)	1.31	0.15	357
Fe ₂ /W(001)	-0.07	0.10	205
Cr ₂ /Pt(001)	-5.74	0.10	175
Mn ₂ /Pt(001)	-2.31	0.14	180
Fe ₂ /Pt(001)	2.49	1.20	7

TABLE I. The table shows the values of J_{12} and $D_{12} = |\vec{D}_{12}|$ (mRy) calculated from their respective ground state. The ground state is represented showing the highest angle between the magnetic moments, i.e. ($\theta > 180$ means that the magnetic moments are pointing inwards.)

C. From local to global representation

The spin Hamiltonian, commonly known as the Heisenberg Hamiltonian is described by a set of parameters which are expected to be sufficient to describe the whole energy landscape of a given system, in a way that the total energy is a function of the magnetic moment directions only, \vec{e}_i , as described in Eq. 1.1. There are several works in the literature where a simple bilinear spin Hamiltonian is not enough to describe the

total energy, therefore, high-order terms are needed as a correction to the Hamiltonian. For instance, for a simple dimer, the total energy, if only the isotropic exchange is considered, should be described as a function of $\cos(\theta)$ as $E_{\text{dimer}} = -J \cos(\theta)$, where J is the isotropic exchange and θ is the angle between the magnetic moments of the atoms. In some situations, such as in Ref. [30], terms as $\cos^2(\theta)$ are important. Therefore, the energy is better described as $E_{\text{dimer}} = -J_1 \cos(\theta) - J_2 \cos^2(\theta)$, where J_2 is now a bi-quadratic term. This was also the case found for an Fe dimer [10, 14], chiral bi-quadratic pair interaction [29] and more complex systems such as an Fe monolayer on Ir(111) [31]. Physically, it means that electrons are hopping between multiple sites giving rise to multi-spin interactions, which is usually the case for itinerant magnets. Therefore, to find the correct Hamiltonian can be a complicated task. The concept of a local Hamiltonian is discussed in Refs. [1, 11, 13] which relies on the magnetic parameters calculated from a given magnetic reference state. With this approach it is necessary to integrate the magnetic interactions to be able to access the global energy landscape. The magnetic interactions are, in this description, a function of the magnetic texture of the system. The positive aspect of this approach is that only a bilinear Hamiltonian is needed. In Appendix B, we demonstrate how the local and global descriptions relate to each other. For the purpose of the present work, we write explicitly how the bilinear DMI can be expressed as a combination of multi-spin interactions as

$$D_{\text{non-col}} = \sin \theta \sum_{n=0, N} a_n \cos^n \theta \quad (3.2)$$

$$D_{\text{SOC}} = \sum_{n=0, N} b_n \cos^n \theta, \quad (3.3)$$

where θ is the angle between the two magnetic moments of the sites being considered, a_n and b_n are the multi-spin parameters and N is the multi-spin index, e.g., $N = 0$ is the bilinear case, $N = 1$ is the biquadratic case and so on. It can be seen from Eqs. 3.2 and 3.3 that for the bilinear case, $N = 0$, the D_{SOC} boils down to a_0 which is essentially the bilinear DMI. Still for $N = 0$, the $D_{\text{non-col}}$ is null if the magnetic moments are aligned in a collinear fashion and only finite if the magnetic moments are non-collinear. We have considered $N = 6$, then fitted the results of our DFT calculations with Eqs. 3.2 and 3.3 and the results are shown in Fig. 3. The dotted and dashed curves represent the fit where optimal values for the parameters are obtained so that the sum of the squared residuals is minimized, while the full lines are our DFT calculations. We have used two different models, e.g. $N=3$ and $N=6$ in Eqs.3.2 and 3.3. While results with $N=6$ fit well with all examples considered, the fit with $N=3$ is inconsistent. It suggests that it is a hard task to know beforehand which order of multi-spin approach to be used.

IV. CONCLUSION

To summarize, in the present work, we have presented a detailed analysis of the microscopic origin of the

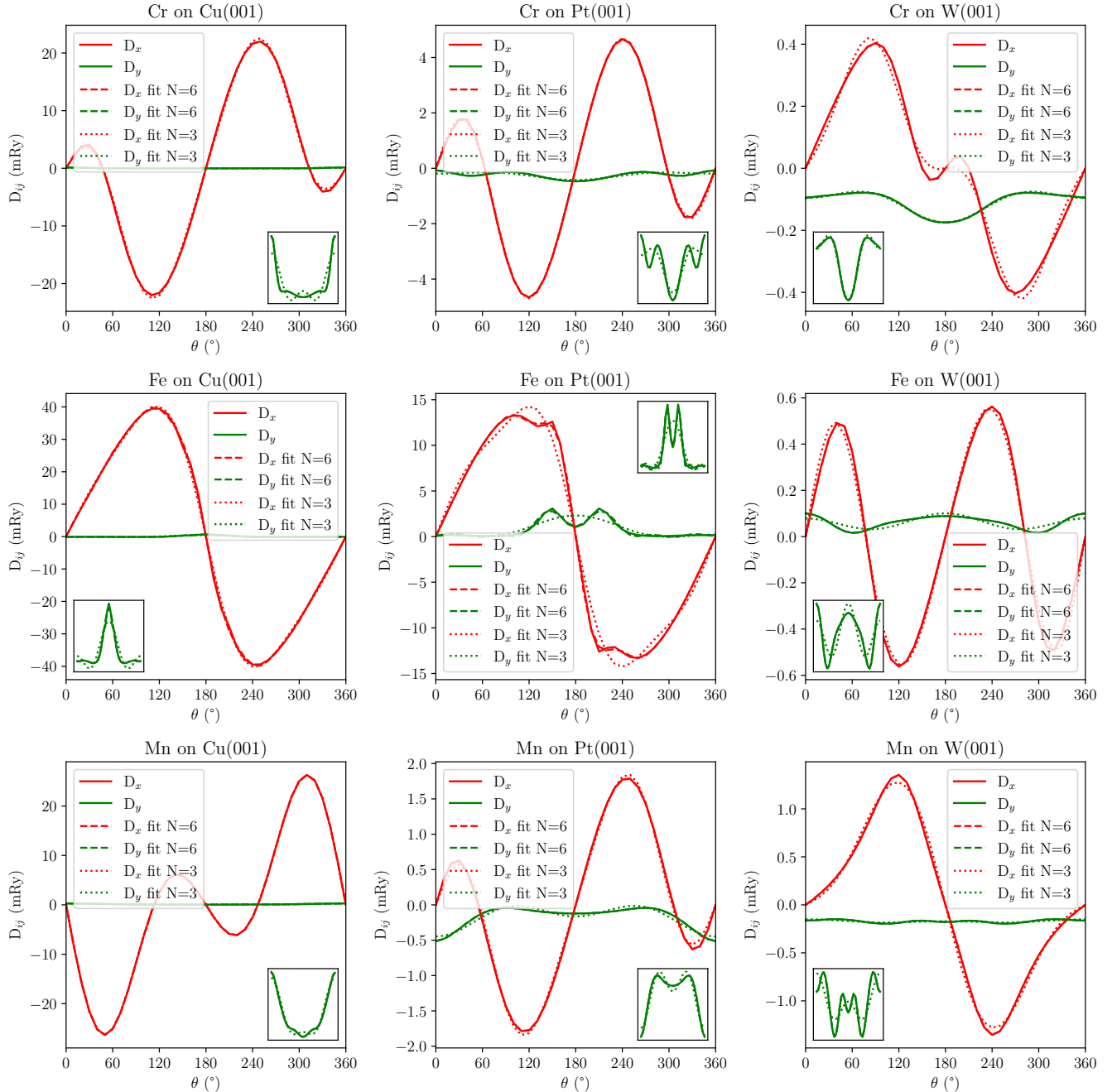


FIG. 3. Fitting the self-consistent calculations (configuration dependent magnetic interactions) with the multi-spin representation (Eqs. 3.2 and 3.3). Here, the full lines are the DFT calculations for the DMI when the spin-orbit coupling is included, while the dashed and dotted curves represent the fitted results of the DFT calculations for $N=3$ and 6 , respectively, using Eqs. 3.2 and 3.3. Note that in the presented examples, the full line and the dashed line are almost indistinguishable while the dotted lines are slightly off and not a good fit in some cases.

Dzyaloshinskii-Moriya (DM) and the DM-like exchange interaction that arises from noncollinear magnetic configuration. We show that while both depend on the spin-orbit coupling (SOC), the former is only finite under the presence of SOC and the latter is finite without SOC but only under non-collinear magnetism. To quantify the analysis, we calculated the electronic structure of dimers (Cr, Fe and Mn) on Pt(001),

W(001), and Cu(001) surfaces using the first principles RSLMTO-ASA method. Based on these calculations, we computed the DMI for various magnetic configurations. Firstly, by employing a formalism that enables the separation of the DMI contributions distinguishing spin- and charge-current-induced DMI terms, we have clarified that the usual spin-orbit driven DMI component is induced by the spin-current generated by

the spin-orbit coupling, and the non-relativistic DM-like component is induced by the non-collinearity of the magnetic moments. Given the absence of the chiral behavior of the DM-like interaction, it is possible to conclude that it gives no contribution to the global energy landscape of the system, unlike the usual DMI.

We also addressed the discussion about the understanding of the spin Hamiltonian and the connection between magnetic-configuration dependent interactions and a multi-spin approach, showing that both are complementary. By doing so, we explicitly show that the magnetic-configuration dependence of these interactions can be mapped onto multi-spin parameters that are independent of the underlying magnetic configuration. The caveat of using the latter approach is that the complete set of parameters is not defined a priori. For instance, we suggest that if one is to perform spin dynamics using a bilinear spin Hamiltonian, the magnetic parameters should be updated following the new magnetic configuration at every time step. In order to avoid this constant update, one should use the spin Hamiltonian with all the relevant multi-spin interactions. To be able to find the latter can be a tricky job, although bilinear and bi-quadratic interactions are dominant in most of the systems studied in the literature. Most likely, systems that present a complex magnetic texture, such as skyrmions, as a ground state are strong candidates to have finite and important multi-spin interactions. Our findings shed light on the underlying mechanisms of the Dzyaloshinskii-Moriya interactions and provide insights into the design and control of magnetic materials for spintronics applications.

V. ACKNOWLEDGEMENTS

R.C acknowledge financial support from FAPERJ - Fundação Carlos Chagas Filho de Amparo à Pesquisa do Estado do Rio de Janeiro, grant number E-26/205.956/2022 and 205.957/2022 (282056). A.B.K. and J.S.S. acknowledge financial support from CAPES and CNPq Brazil. A.B.K. acknowledges the INCT of Materials Informatics. Valuable discussions with Dr. Danny Thonig and Prof. Mikhail Katsnelson are acknowledged. O.E. acknowledges support from the Swedish Research Council (VR), the European Research Council (ERC, FASTCORR project), the Knut and Alice Wallenberg Foundation (KAW) and STandUPP. O.E. and A. B. acknowledge financial support from eSENCE. A.D. acknowledges financial support from Financial support from Vetenskapsrådet (grant numbers VR 2016-05980 and VR 2019-05304), and the Knut and Alice Wallenberg foundation (grant numbers 2018.0060, 2021.0246, and 2022.0108). The computations were enabled by resources provided by the computational facilities of the CCAD/UFPA (Brazil), at the National Laboratory for Scientific Computing (LNCC/MCTI, Brazil) as well as the National Academic Infrastructure for Supercomputing in Sweden (NAISS) and the Swedish National Infrastructure for Computing (SNIC) at NSC and PDC, partially funded by the Swedish Research Council through grant agreements no. 2022-06725 and no. 2018-05973. J.F. acknowledges support from Vetenskapsrådet and Stiftelsen Olle En-

gkvist Byggmästare.

Appendix A: Analytical model dimer

1. Defects on a metallic surface

We assume a simple two-dimensional electron gas, e.g., surface states on a metallic surface with a Rashba spin-orbit coupling, in which magnetic defects are embedded. We model this system by the Hamiltonian

$$\mathcal{H} = \sum_{\mathbf{k}} \Psi_{\mathbf{k}}^{\dagger} \epsilon_{\mathbf{k}} \Psi_{\mathbf{k}} + \int \Psi^{\dagger}(\mathbf{r}) \mathbf{V}(\mathbf{r}) \Psi(\mathbf{r}) d\mathbf{r}, \quad (\text{A1})$$

where the spinor $\Psi_{\mathbf{k}} = (c_{\mathbf{k}\uparrow} \ c_{\mathbf{k}\downarrow})^t$ ($\Psi_{\mathbf{k}}^{\dagger} = (c_{\mathbf{k}\uparrow}^{\dagger} \ c_{\mathbf{k}\downarrow}^{\dagger})$) denotes the annihilation (creation) operator for electrons with energy $\epsilon_{\mathbf{k}} = \epsilon_{\mathbf{k}}\sigma^0 + \alpha[\mathbf{k} \times \hat{\mathbf{z}}] \cdot \boldsymbol{\sigma}$ at the momentum \mathbf{k} , spin $\sigma = \uparrow, \downarrow$, and Rashba coupling strength α . Moreover, the $\Psi(\mathbf{r}) = \int \Psi_{\mathbf{k}} e^{-i\mathbf{k}\cdot\mathbf{r}} d\mathbf{k}/\Omega$ and $\Psi^{\dagger}(\mathbf{r}) = \int \Psi_{\mathbf{k}}^{\dagger} e^{i\mathbf{k}\cdot\mathbf{r}} d\mathbf{k}/\Omega$ are the corresponding coordinate space operators, where Ω is the integration volume, whereas the scattering potential $\mathbf{V}(\mathbf{r}) = \sum_m \mathbf{V}_m \delta(\mathbf{r} - \mathbf{r}_m)$ defines a collection of defects $\mathbf{V}_m = V_m \sigma^0 + \mathbf{m}_m \cdot \boldsymbol{\sigma}$.

2. Green function

In this model, the unperturbed retarded Green function (GF) $\mathbf{g}_{\mathbf{k}}$ is defined for the first term of Eq. (A1), and is given in reciprocal and real space by the expressions

$$\mathbf{g}_{\mathbf{k}}(z) = \frac{(z - \epsilon_{\mathbf{k}})\sigma^0 + \alpha[\mathbf{k} \times \hat{\mathbf{z}}] \cdot \boldsymbol{\sigma}}{(z - \epsilon_{\mathbf{k}})^2 - \alpha^2 k^2}, \quad (\text{A2a})$$

$$\mathbf{g}(\mathbf{r}, \omega) = -i \frac{N_0}{4} \sum_{s=\pm} \frac{\kappa_s}{\kappa} \left(H_0^{(1)}(\kappa_s r) \sigma^0 - is H_1^{(1)}(\kappa_s r) [\hat{\mathbf{r}} \times \hat{\mathbf{z}}] \cdot \boldsymbol{\sigma} \right), \quad (\text{A2b})$$

respectively. These two representations of \mathbf{g} is related via the Fourier transform $\mathbf{g}_{\mathbf{k}} = \int \mathbf{g}(\mathbf{r}) e^{i\mathbf{k}\cdot\mathbf{r}} d\mathbf{r}$. Moreover, we have introduced the notation $\kappa = \sqrt{2N_0(\omega + \epsilon_F - \alpha^2 N_0/2)}$, where ϵ_F denotes the Fermi energy, $\kappa_s = \kappa + s\alpha N_0$, and $N_0 = m/\hbar^2$, whereas $H_m^{(1)}$ is the Hankel function. Also, $k = |\mathbf{k}|$. In this way we have defined $\mathbf{g}_{\mathbf{k}} = g_0 \sigma^0 + \mathbf{g}_1 \cdot \boldsymbol{\sigma}$ in both coordinate and reciprocal space.

The dressed GF \mathbf{G} is calculated by inclusion of the scattering potential \mathbf{V} , c.f., Eq. (A1). The dressed GF can be formulated in terms of the T -matrix expansion of the impurity potential, giving in reciprocal space the expression

$$\mathbf{G}_{\mathbf{k}\mathbf{k}'} = \delta(\mathbf{k} - \mathbf{k}') \mathbf{g}_{\mathbf{k}} + \sum_{mn} \mathbf{g}_{\mathbf{k}} e^{-i\mathbf{k}\cdot\mathbf{r}_m} \mathbf{T}(\mathbf{R}_{mn}) e^{i\mathbf{k}'\cdot\mathbf{r}_n} \mathbf{g}_{\mathbf{k}'}, \quad (\text{A3})$$

where $\mathbf{R}_{mn} = \mathbf{r}_m - \mathbf{r}_n$, whereas the T -matrix is given by

$$\mathbf{T}(\mathbf{R}_{mn}) = \mathbf{V}_m (\mathbf{t}^{-1})_{mn}, \quad (\text{A4a})$$

$$\mathbf{t}_{mn} = \delta_{mn} \sigma^0 - \mathbf{g}(\mathbf{R}_{mn}) \mathbf{V}_n. \quad (\text{A4b})$$

For later purpose, we also define the correction $\delta\mathbf{G}(\mathbf{r}, \mathbf{r}')$ to the Green function in coordinate space (via $\mathbf{G}(\mathbf{r}, \mathbf{r}') = \int \mathbf{G}_{\mathbf{k}\mathbf{k}'} e^{-i\mathbf{k}\cdot\mathbf{r}+i\mathbf{k}'\cdot\mathbf{r}'} d\mathbf{k}d\mathbf{k}'/\Omega^2$) as

$$\delta\mathbf{G}(\mathbf{r}, \mathbf{r}') = \sum_{mn} \mathbf{g}(\mathbf{r} - \mathbf{r}_m) \mathbf{T}(\mathbf{R}_{mn}) \mathbf{g}(\mathbf{r}_n - \mathbf{r}'). \quad (\text{A5})$$

Here, since the scattering potential is partitioned into a non-magnetic and a magnetic component, we can write $\mathbf{T}(\mathbf{R}_{mn}) = T_0(\mathbf{R}_{mn})\sigma^0 + \mathbf{T}_1(\mathbf{R}_{mn}) \cdot \boldsymbol{\sigma}$. We also remark that the potential \mathbf{V}_m should here be considered as an expectation value, such that $\mathbf{V}_m = V_m\sigma^0 + \langle \mathbf{m}_m \rangle \cdot \boldsymbol{\sigma}$.

Next, we show that the T -matrix is not necessarily symmetric under changes of the site order $\mathbf{R}_{mn} \rightarrow \mathbf{R}_{nm}$. For the sake of argument, consider two magnetic impurities on the surface, giving

$$\mathbf{t} = \begin{pmatrix} \sigma^0 - g_0\mathbf{V}_1 & -\mathbf{g}(R_{12})\mathbf{V}_2 \\ -\mathbf{g}(R_{21})\mathbf{V}_1 & \sigma^0 - g_0\mathbf{V}_2 \end{pmatrix}, \quad (\text{A6})$$

where each entry is a 2×2 -matrix. The diagonal components only include g_0 since $\mathbf{g}_1(R_{mm}) \equiv 0$. Moreover, we denote $R_{mn} = |\mathbf{R}_{mn}|$, and $g_0 = g_0(R_{mm})$, whereas we set $g_{mn} = g_0(R_{mn})$, and $\mathbf{g}_{mn} = \mathbf{g}_1(R_{mn})$, for $m \neq n$.

We need the inverse of the matrix \mathbf{t} and, for the sake of

notation, set $\mathbf{s} = \mathbf{t}^{-1}$. Then, we can write

$$\mathbf{s}_1 = \left(\sigma^0 - g_0\mathbf{V}_1 - \mathbf{g}(R_{12})\mathbf{V}_2 (\sigma^0 - g_0\mathbf{V}_1)^{-1} \mathbf{g}(R_{21})\mathbf{V}_1 \right)^{-1}, \quad (\text{A7a})$$

$$\mathbf{s}_{12} = -\mathbf{s}_1 \mathbf{g}(R_{12}) \mathbf{V}_2 (\sigma^0 - g_0\mathbf{V}_2)^{-1}, \quad (\text{A7b})$$

$$\mathbf{s}_{21} = -\mathbf{s}_2 \mathbf{g}(R_{21}) \mathbf{V}_1 (\sigma^0 - g_0\mathbf{V}_1)^{-1}, \quad (\text{A7c})$$

$$\mathbf{s}_2 = \left(\sigma^0 - g_0\mathbf{V}_2 - \mathbf{g}(R_{21})\mathbf{V}_1 (\sigma^0 - g_0\mathbf{V}_2)^{-1} \mathbf{g}(R_{12})\mathbf{V}_2 \right)^{-1}. \quad (\text{A7d})$$

These expressions can be simplified, without loosing any essential features pertaining to the symmetries of the T -matrix, by assuming that

$$\left\| \mathbf{g}(R_{12})\mathbf{V}_n (\sigma^0 - g_0\mathbf{V}_m)^{-1} \mathbf{g}(R_{21})\mathbf{V}_m \right\| \ll \left\| \sigma^0 - g_0\mathbf{V}_m \right\|. \quad (\text{A8})$$

This assumption can be achieved by locating the impurities at a sufficiently large distance from each another. We also assume that the impurities constitute a purely magnetic scattering potential, hence, $V_m = 0$. Then, \mathbf{s} reduces to

$$\mathbf{s}_1 = \left(\sigma^0 - g_0 \langle \mathbf{m}_1 \rangle \cdot \boldsymbol{\sigma} \right)^{-1} = \frac{\sigma^0 + g_0 \langle \mathbf{m}_1 \rangle \cdot \boldsymbol{\sigma}}{1 - g_0^2 |\mathbf{m}_1|^2}, \quad (\text{A9a})$$

$$\mathbf{s}_{12} = -\mathbf{g}(R_{12}) \frac{\sigma^0 + g_0 \langle \mathbf{m}_1 \rangle \cdot \boldsymbol{\sigma}}{1 - g_0^2 |\mathbf{m}_1|^2} \langle \mathbf{m}_2 \rangle \cdot \boldsymbol{\sigma} \frac{\sigma^0 + g_0 \langle \mathbf{m}_2 \rangle \cdot \boldsymbol{\sigma}}{1 - g_0^2 |\mathbf{m}_2|^2}, \quad (\text{A9b})$$

$$\mathbf{s}_{21} = -\mathbf{g}(R_{21}) \frac{\sigma^0 + g_0 \langle \mathbf{m}_2 \rangle \cdot \boldsymbol{\sigma}}{1 - g_0^2 |\mathbf{m}_2|^2} \langle \mathbf{m}_1 \rangle \cdot \boldsymbol{\sigma} \frac{\sigma^0 + g_0 \langle \mathbf{m}_1 \rangle \cdot \boldsymbol{\sigma}}{1 - g_0^2 |\mathbf{m}_1|^2}, \quad (\text{A9c})$$

$$\mathbf{s}_2 = \frac{\sigma^0 + g_0 \langle \mathbf{m}_2 \rangle \cdot \boldsymbol{\sigma}}{1 - g_0^2 |\mathbf{m}_2|^2}. \quad (\text{A9d})$$

It is clear that $\mathbf{s}_{12} \neq \mathbf{s}_{21}$ and, hence, $\mathbf{T}(\mathbf{R}_{mn}) \neq \mathbf{T}(\mathbf{R}_{nm})$ whenever $\langle \mathbf{m}_1 \rangle \cdot \boldsymbol{\sigma} \neq \langle \mathbf{m}_2 \rangle \cdot \boldsymbol{\sigma}$. For a simpler notation, below we shall write \mathbf{m}_m instead of $\langle \mathbf{m}_m \rangle$.

The critical components of the off-diagonal T -matrix elements are the numerators since the denominators are equal in the two elements. In the given notation, one derives for $m \neq n$

$$\begin{aligned} \mathbf{T}(\mathbf{R}_{mn}) &\sim \mathbf{m}_m \cdot \boldsymbol{\sigma} (\sigma^0 + g_0 \mathbf{m}_m \cdot \boldsymbol{\sigma}) \mathbf{g}(R_{mn}) \mathbf{m}_n \cdot \boldsymbol{\sigma} (\sigma^0 + g_0 \mathbf{m}_n \cdot \boldsymbol{\sigma}) \\ &= \left\{ g_{mn} (g_0^2 m_m^2 m_n^2 + \mathbf{m}_m \cdot \mathbf{m}_n) + \mathbf{g}_{mn} \cdot \left[g_0 (\mathbf{m}_m m_n^2 + m_m^2 \mathbf{m}_n) - i \mathbf{m}_m \times \mathbf{m}_n \right] \right\} \sigma^0 \\ &\quad + \left\{ g_0^2 m_m^2 m_n^2 \mathbf{g}_{mn} + g_0 g_{mn} (m_n^2 \mathbf{m}_m + m_m^2 \mathbf{m}_n) + \mathbf{m}_m \cdot \mathbf{g}_{mn} \mathbf{m}_n + \mathbf{m}_m \mathbf{g}_{mn} \cdot \mathbf{m}_n - \mathbf{m}_m \cdot \mathbf{m}_n \mathbf{g}_{mn} \right. \\ &\quad \left. - i g_0 \mathbf{g}_{mn} \times (\mathbf{m}_m m_n^2 - m_m^2 \mathbf{m}_n) + i g_{mn} \mathbf{m}_m \times \mathbf{m}_n \right\} \cdot \boldsymbol{\sigma}. \end{aligned} \quad (\text{A10})$$

Using these explicit expressions for the T -matrix, the charge and spin density components G_{01} and \mathbf{G}_{10} , and the corresponding current components G_{01} and \mathbf{G}_{11} can be identified from the charge and spin components G_0 and \mathbf{G}_1 , respectively. The two-index notation refers to the charge and spin densities G_{00} and \mathbf{G}_{10} , and the charge and spin currents G_{10} and \mathbf{G}_{11} .

In doing so, first identify the components in the T -matrix, Eq. (A10), that are even and odd under $\mathbf{R}_{mn} \rightarrow \mathbf{R}_{nm}$, using the

properties $g_0(-\mathbf{r}) = g_0(\mathbf{r})$ while $\mathbf{g}_1(-\mathbf{r}) = -\mathbf{g}_1(\mathbf{r})$. Hence, adopting the two-index notation, the four components to the T -matrix are summarized as

$$T_{00}(\mathbf{R}_{mn}) = g_{mn}(g_0^2 m_m^2 m_n^2 + \mathbf{m}_m \cdot \mathbf{m}_n) - i\mathbf{g}_{mn} \cdot (\mathbf{m}_m \times \mathbf{m}_n), \quad (\text{A11a})$$

$$T_{01}(\mathbf{R}_{mn}) = g_0 \mathbf{g}_{mn} \cdot (\mathbf{m}_m m_n^2 + m_m^2 \mathbf{m}_n), \quad (\text{A11b})$$

$$\mathbf{T}_{10}(\mathbf{R}_{mn}) = g_0 g_{mn} (m_n^2 \mathbf{m}_m + m_m^2 \mathbf{m}_n) - i g_0 \mathbf{g}_{mn} \times (\mathbf{m}_m m_n^2 - m_m^2 \mathbf{m}_n), \quad (\text{A11c})$$

$$\mathbf{T}_{11}(\mathbf{R}_{mn}) = g_0^2 m_m^2 m_n^2 \mathbf{g}_{mn} + i g_{mn} \mathbf{m}_m \times \mathbf{m}_n + \mathbf{m}_m \cdot \mathbf{g}_{mn} \mathbf{m}_n + \mathbf{m}_m \mathbf{g}_{mn} \cdot \mathbf{m}_n - \mathbf{m}_m \cdot \mathbf{m}_n \mathbf{g}_{mn}. \quad (\text{A11d})$$

With reference to these expressions, and using the notation $\mathbf{R}_m = \mathbf{r} - \mathbf{r}_m$, define the formal expressions

$$\begin{aligned} \delta G_{00}(\mathbf{r}, \mathbf{r}') = \sum_{mn} & \left(T_{00}(\mathbf{R}_{mn}) (g_0(\mathbf{R}_m) g_0(\mathbf{R}_n) - \mathbf{g}_1(\mathbf{R}_m) \cdot \mathbf{g}_1(\mathbf{R}_n)) - g_0(\mathbf{R}_m) \mathbf{T}_{11}(\mathbf{R}_{mn}) \cdot \mathbf{g}_1(\mathbf{R}_n) - \mathbf{g}_1(\mathbf{R}_m) \cdot \mathbf{T}_{11}(\mathbf{R}_{mn}) g_0(\mathbf{R}_n) \right. \\ & \left. - i(\mathbf{g}_1(\mathbf{R}_m) \times \mathbf{T}_{11}(\mathbf{R}_{mn})) \cdot \mathbf{g}_1(\mathbf{R}_n) \right), \end{aligned} \quad (\text{A12a})$$

$$\begin{aligned} \delta G_{01}(\mathbf{r}, \mathbf{r}') = \sum_{mn} & \left(T_{01}(\mathbf{R}_{mn}) (g_0(\mathbf{R}_m) g_0(\mathbf{R}_n) - \mathbf{g}_1(\mathbf{R}_m) \cdot \mathbf{g}_1(\mathbf{R}_n)) - g_0(\mathbf{R}_m) \mathbf{T}_{10}(\mathbf{R}_{mn}) \cdot \mathbf{g}_1(\mathbf{R}_n) + \mathbf{g}_1(\mathbf{R}_m) \cdot \mathbf{T}_{10}(\mathbf{R}_{mn}) g_0(\mathbf{R}_n) \right. \\ & \left. - i(\mathbf{g}_1(\mathbf{R}_m) \times \mathbf{T}_{10}(\mathbf{R}_{mn})) \cdot \mathbf{g}_1(\mathbf{R}_n) \right), \end{aligned} \quad (\text{A12b})$$

$$\begin{aligned} \delta \mathbf{G}_{10}(\mathbf{r}, \mathbf{r}') = \sum_{mn} & \left(T_{01}(\mathbf{R}_{mn}) (\mathbf{g}_1(\mathbf{R}_m) g_0(\mathbf{R}_n) - g_0(\mathbf{R}_m) \mathbf{g}_1(\mathbf{R}_n) - i\mathbf{g}_1(\mathbf{R}_m) \times \mathbf{g}_1(\mathbf{R}_n)) + \mathbf{T}_{10} (g_0(\mathbf{R}_m) g_0(\mathbf{R}_n) + \mathbf{g}_1(\mathbf{R}_m) \cdot \mathbf{g}_1(\mathbf{R}_n)) \right. \\ & \left. - \mathbf{g}_1(\mathbf{R}_m) \mathbf{T}_{10}(\mathbf{R}_{mn}) \cdot \mathbf{g}_1(\mathbf{R}_n) - \mathbf{g}_1(\mathbf{R}_m) \cdot \mathbf{T}_{10}(\mathbf{R}_{mn}) \mathbf{g}_1(\mathbf{R}_n) + i\mathbf{g}_1(\mathbf{R}_m) \times \mathbf{T}_{10}(\mathbf{R}_{mn}) g_0(\mathbf{R}_n) - i g_0(\mathbf{R}_m) \mathbf{T}_{10}(\mathbf{R}_{mn}) \times \mathbf{g}_1(\mathbf{R}_n) \right), \end{aligned} \quad (\text{A12c})$$

$$\begin{aligned} \delta \mathbf{G}_{11}(\mathbf{r}, \mathbf{r}') = \sum_{mn} & \left(T_{00}(\mathbf{R}_{mn}) (\mathbf{g}_1(\mathbf{R}_m) g_0(\mathbf{R}_n) - g_0(\mathbf{R}_m) \mathbf{g}_1(\mathbf{R}_n) - i\mathbf{g}_1(\mathbf{R}_m) \times \mathbf{g}_1(\mathbf{R}_n)) + \mathbf{T}_{11}(\mathbf{R}_{mn}) (g_0(\mathbf{R}_m) g_0(\mathbf{R}_n) + \mathbf{g}_1(\mathbf{R}_m) \cdot \mathbf{g}_1(\mathbf{R}_n)) \right. \\ & \left. - \mathbf{g}_1(\mathbf{R}_m) \mathbf{T}_{11}(\mathbf{R}_{mn}) \cdot \mathbf{g}_1(\mathbf{R}_n) - \mathbf{g}_1(\mathbf{R}_m) \cdot \mathbf{T}_{11}(\mathbf{R}_{mn}) \mathbf{g}_1(\mathbf{R}_n) + i\mathbf{g}_1(\mathbf{R}_m) \times \mathbf{T}_{11}(\mathbf{R}_{mn}) g_0(\mathbf{R}_n) - i g_0(\mathbf{R}_m) \mathbf{T}_{11}(\mathbf{R}_{mn}) \times \mathbf{g}_1(\mathbf{R}_n) \right). \end{aligned} \quad (\text{A12d})$$

3. Anti-symmetric anisotropy

In Ref. [26], a general expression for the Dzyaloshinskii-Moriya-like interaction $\mathbf{D}(\mathbf{r}, \mathbf{r}')$ between two spins located at \mathbf{r} and \mathbf{r}' , respectively was derived, here repeated for convenience,

$$\begin{aligned} \mathbf{D}(\mathbf{r}, \mathbf{r}') \sim v^2 \text{Re} \int f(\omega) & \{ G_{01}(\mathbf{r}, \mathbf{r}') \mathbf{G}_{10}(\mathbf{r}', \mathbf{r}) \\ & + G_{00}(\mathbf{r}, \mathbf{r}') \mathbf{G}_{11}(\mathbf{r}', \mathbf{r}) \} d\omega. \end{aligned} \quad (\text{A13})$$

In this expression, v denotes the local exchange interaction between the electron spin and the localized magnetic moment, while $f(\omega)$ is the Fermi-Dirac distribution function. Then, using the example discussed here, it is easy to see that this interaction has a non-vanishing component also in the absence of \mathbf{g}_1 . Since any kind of spin texture, e.g., spin-polarization or spin-orbit coupling, in the unperturbed electronic structure is accounted for by \mathbf{g}_1 , this implies that there may arise a non-vanishing Dzyaloshinskii-Moriya-like contribution to the spin-spin interactions also for a trivial spin-degenerate electron gas. Indeed, whenever $\mathbf{g}_1 = 0$, the above derivation leads to that

$\delta G_{01}(\mathbf{r}, \mathbf{r}') = 0$ and

$$\begin{aligned} \delta \mathbf{G}_{11}(\mathbf{r}, \mathbf{r}') &= \sum_{mn} g_0(\mathbf{r} - \mathbf{r}_m) \mathbf{T}_1(\mathbf{R}_{mn}) g_0(\mathbf{r}_n - \mathbf{r}') \\ &= i \sum_{mn} \frac{g_0(\mathbf{r} - \mathbf{r}_m) g_0(\mathbf{R}_{mn}) g_0(\mathbf{r}_n - \mathbf{r}')}{(1 - g_0^2 |\mathbf{m}_m|^2)(1 - g_0^2 |\mathbf{m}_n|^2)} \mathbf{m}_m \times \mathbf{m}_n. \end{aligned} \quad (\text{A14})$$

Hence, taking $G_{00} \approx g_0$, we obtain

$$\begin{aligned} \mathbf{D}(\mathbf{r}, \mathbf{r}') &= \frac{N_0^3}{4\pi} \text{Re} \sum_{mn} \mathbf{m}_m \times \mathbf{m}_n \int f(\omega) H_0^{(1)}(\kappa|\mathbf{r} - \mathbf{r}'|) \\ &\quad \times \frac{H_0^{(1)}(\kappa|\mathbf{r}' - \mathbf{r}_m|) H_0^{(1)}(\kappa|\mathbf{r} - \mathbf{r}_n|)}{(1 + N_0^2 |\mathbf{m}_m|^2 / 2)(1 + N_0^2 |\mathbf{m}_n|^2 / 4)} d\omega, \end{aligned} \quad (\text{A15})$$

showing the existence of a non-vanishing Dzyaloshinskii-Moriya interaction between spin moments whenever they are in a non-collinear configuration. Moreover, using this example, we notice that this interaction is non-vanishing for collinear spin moments in presence of an intrinsic spin texture.

In Ref. [32], chiral molecules were adsorbed onto Cu and Au surfaces, resulting in strongly modified effective spin-orbit coupling and ferromagnetism, respectively, in the two

compounds. The magnetic properties associated with the composite structure of chiral molecules interfaced with metals were suggested to result from the type of impurity induced Dzyaloshinskii-Moriya-like interaction formulated in Eq. (A15).

Appendix B: Decomposition of spin-current Green functions.

As explained in Refs. 16, 15 and 1 there exist sum rules which the self-consistent Green function has to fulfill. Here we sketch the most relevant relations arising from such sum rules for a magnetic dimer on a non-magnetic substrate, while the details will be presented in a coming report. Further, we divide the terms into having non-relativistic (n) or relativistic (r) origin, based on whether they are independent of spin-orbit coupling or not. First, we have the two most important terms for the time reversal odd and non-relativistic part of the \vec{G}^0 Green function

$$\vec{G}_{ik}^{0n} \approx - \sum_j \left\{ G_{ij}^{00} \vec{B}_j G_{jk}^{00} - \vec{G}_{ij}^{0n} \vec{B}_j \cdot \vec{G}_{jk}^{0n} \right\}, \quad (\text{B1})$$

Then, we have a corresponding sum rule for the time reversal even spin dependent spin current related Green function, \vec{G}^1 , where the most important non-relativistic and relativistic contributions, respectively, take the form

$$\vec{G}_{il}^{1n} \approx \sum_{jk} i \vec{G}_{ij}^{0n} \times \lambda_{jk} \vec{G}_{kl}^{0n} \quad (\text{B2})$$

$$\vec{G}_{il}^{1r} \approx - \sum_{jk} \left\{ G_{ij}^{00} \vec{\xi}_{jk} G_{kl}^{00} + \left(\vec{G}_{ij}^{0n} \times \vec{\xi}_{jk} \right) \times \vec{G}_{kl}^{0n} \right\}, \quad (\text{B3})$$

with

$$\lambda_{jk} = \frac{1}{2} \text{Tr}_s \left(G_{jk}^{0-1} + \Delta V_j \delta_{jk} \right) \quad (\text{B4})$$

$$\vec{\xi}_{jk} = \frac{1}{2} \text{Tr}_s \vec{\sigma} \left(G_{jk}^{0-1} + \Delta V_j \delta_{jk} \right), \quad (\text{B5})$$

where the latter is spin dependent due to the fact that it is directly proportional to the spin-orbit coupling. Now we can systematically substitute the \vec{G}^{0n} factors in Eqs. (B2) and (B3) by the terms in Eq. (B1). In the first iterations this leads to

$$\begin{aligned} \vec{G}_{ij}^{1n} &\approx i \sum_{kl} \vec{G}_{ik}^{0n} \times \lambda_{kl} \vec{G}_{lj}^{0n} = \\ &\approx i \sum_{klmn} \left(G_{ik}^{00} \vec{B}_k G_{kl}^{00} - \vec{G}_{ik}^{0n} \vec{B}_k \cdot \vec{G}_{kl}^{0n} \right) \times \lambda_{lm} \left(G_{mn}^{00} \vec{B}_n G_{nj}^{00} - \vec{G}_{lm}^{0n} \vec{B}_m \cdot \vec{G}_{mj}^{0n} \right) = \\ &= i \sum_{klmn} G_{ik}^{00} \vec{B}_k G_{kl}^{00} \times \lambda_{lm} G_{mn}^{00} \vec{B}_n G_{nj}^{00} + \\ &- i \sum_{klmnpq} \left\{ G_{ik}^{00} \vec{B}_k G_{kp}^{00} \left(\vec{B}_p G_{pq}^{00} \cdot \vec{B}_q G_{ql}^{00} \right) \times \lambda_{lm} G_{mn}^{00} \vec{B}_n G_{nj}^{00} + G_{ik}^{00} \vec{B}_k G_{kl}^{00} \times \lambda_{lm} G_{mn}^{00} \vec{B}_n G_{np}^{00} \left(\vec{B}_p G_{pq}^{00} \cdot \vec{B}_q G_{qj}^{00} \right) \right\} + \\ &+ i \sum_{klmnpqrs} G_{ik}^{00} \vec{B}_k G_{kp}^{00} \left(\vec{B}_p G_{pq}^{00} \cdot \vec{B}_q G_{ql}^{00} \right) \times \lambda_{lm} G_{mn}^{00} \vec{B}_n G_{nr}^{00} \left(\vec{B}_r G_{rs}^{00} \cdot \vec{B}_s G_{sj}^{00} \right) = \\ &= \left\{ A_0 + A_1 (\hat{m}_1 \cdot \hat{m}_2) + A_2 (\hat{m}_1 \cdot \hat{m}_2)^2 \right\} (\hat{m}_1 \times \hat{m}_2), \end{aligned} \quad (\text{B6})$$

where the prefactors A_i are in general linear combinations of multi-spin products, whose forms are obtained by iterations that identify the non-vanishing multi-spin terms with lowest number of spins, respectively

$$\begin{aligned} \vec{G}_{ij}^{1r} &\approx - \sum_{kl} G_{ik}^{00} \vec{\xi}_{kl} G_{lj}^{00} - \sum_{klmn} \left\{ \left(G_{im}^{00} \vec{B}_m G_{mk}^{00} - \vec{G}_{im}^{0n} \vec{B}_m \cdot \vec{G}_{mk}^{0n} \right) \times \vec{\xi}_{kl} \right\} \times \left(G_{ln}^{00} \vec{B}_n G_{nj}^{00} - \vec{G}_{ln}^{0n} \vec{B}_n \cdot \vec{G}_{nj}^{0n} \right) = \\ &= - \sum_{kl} G_{ik}^{00} \vec{\xi}_{kl} G_{lj}^{00} - \sum_{klmn} G_{im}^{00} \vec{B}_m G_{mk}^{00} \vec{\xi}_{kl} G_{ln}^{00} \vec{B}_n G_{nj}^{00} + \\ &+ \sum_{klmnpq} \left\{ G_{im}^{00} \vec{B}_m G_{mp}^{00} \left(\vec{B}_p G_{pq}^{00} \cdot \vec{B}_q G_{qk}^{00} \right) \vec{\xi}_{kl} G_{ln}^{00} \vec{B}_n G_{nj}^{00} + G_{im}^{00} \vec{B}_m G_{mk}^{00} \vec{\xi}_{kl} G_{ln}^{00} \vec{B}_n G_{np}^{00} \left(\vec{B}_p G_{pq}^{00} \cdot \vec{B}_q G_{qj}^{00} \right) \right\} + \\ &- \sum_{klmnpqrs} G_{im}^{00} \vec{B}_m G_{mp}^{00} \left(\vec{B}_p G_{pq}^{00} \cdot \vec{B}_q G_{qk}^{00} \right) \vec{\xi}_{kl} G_{ln}^{00} \vec{B}_n G_{nr}^{00} \left(\vec{B}_r G_{rs}^{00} \cdot \vec{B}_s G_{sj}^{00} \right) = \\ &= \left(B_0 + B_1 (\hat{m}_1 \cdot \hat{m}_2) + B_2 (\hat{m}_1 \cdot \hat{m}_2)^2 \right) \hat{\xi}, \end{aligned} \quad (\text{B7})$$

where the prefactors B_i are again multi-spin products. The site summations of Eqs. (B6) and (B7) lead uniquely to the

final reference dependence only when there are no intersite Green functions in the product. Intra-site Green func-

tions can lead to trivial factors, such as $\hat{m}_1 \cdot \hat{m}_1 = 1$. For instance, the third and fourth terms in Eq. (B7) contributes to a constant B_0 for those terms where $p = q$, but to B_1 when $p \neq q$. Now, we can substitute the G^{\uparrow} factor in the first term of the Dzyaloshinskii-Moriya interaction in Eq. (2.6) by the relations of Eqs. (B6) and (B7) and by integrating and summing over multi-spin paths for the factors A_i and B_i we obtain the interactions strength given by a_i and b_i in Eq. (3.2) and (3.3). For a dimer in the geometry of Fig. 1 we have also found that there are two independent contributions to the Dzyaloshinskii-Moriya like interaction. In addition to the fact that the reference state dependence is different, the Dzyaloshinskii-Moriya vector points out of magnetic plane for the non-relativistic contribution while it points along $\hat{\xi} = \hat{y}$ axis for the relativistic contribution as specified by the Moriya symmetry rules.

Appendix C: Details of the DFT calculations

The electronic structure calculations were performed using the first-principles, self-consistent real space - linear muffin tin orbital - atomic sphere approximation (RS-LMTO-ASA) method [21, 22, 33–43], which has been generalized to the treatment of non-collinear magnetism [24, 25]. This method is based on the LMTO-ASA formalism [44], and solves the eigenvalue problem directly in real space using the Haydock

recursion method [45]. The local spin density approximation (LSDA) was employed for the exchange-correlation energy [46]. To terminate the continued fraction that arises in the recursion method, we used the Beer-Pettifor terminator [47] after 21 recursion levels. The spin-orbit coupling interaction was included by adding a term $\xi L \cdot S$ to the Kohn-Sham Hamiltonian, where ξ was calculated self-consistently at each variational step. When calculations without spin-orbit coupling are mentioned in the text, it means that ξ was set to zero after the self-consistent calculation.

Here, we have considered Cr, Fe, and Mn dimers supported on Cu(001), Pt(001), and W(001) surfaces. The Cu and Pt substrates were simulated by a cluster containing ~ 15000 atoms located in an fcc lattice with the experimental lattice parameter of Cu and Pt, respectively. The W surface was treated analogously using a bcc lattice. In order to provide a basis for the wave function near the surface and to handle charge transfers accurately, we included two overlayers of empty spheres above the surface layer. The calculations of the dimers were performed by embedding the clusters as a perturbation on the self-consistently converged surfaces. The dimer sites and those of the closest shell of Cu, Pt, W, or empty spheres sites around the defect were recalculated self-consistently, while the electronic structure for all other sites remained unchanged at their clean surface values. Lattice relaxations were neglected in the systems considered in this study.

-
- [1] A. Szilva, Y. Kvashnin, E. A. Stepanov, L. Nordström, O. Eriksson, A. I. Liechtenstein, and M. I. Katsnelson, “Quantitative theory of magnetic interactions in solids,” (2022), number: arXiv:2206.02415 arXiv:2206.02415 [cond-mat].
 - [2] H. Yang, J. Liang, and Q. Cui, *Nature Reviews Physics* **5**, 43 (2023).
 - [3] A. Jacobsson, G. Johansson, I. Gorbatov, O., M. Lezaic, B. Sanyal, S. Blugel, and C. Etz, *Scientific Reports* **12**, 18987 (2022), 10.1038/s41598-022-20311-7.
 - [4] S. Mankovsky, S. Polesya, and H. Ebert, *Phys. Rev. B* **101**, 174401 (2020).
 - [5] S. Mankovsky, S. Polesya, and H. Ebert, *Phys. Rev. B* **104**, 054418 (2021).
 - [6] A. I. Liechtenstein, M. I. Katsnelson, V. P. Antropov, and V. A. Gubanov, *Journal of Magnetism and Magnetic Materials* **67**, 65 (1987).
 - [7] A. I. Liechtenstein, M. I. Katsnelson, and V. A. Gubanov, *J. Phys. F: Met. Phys.* **14**, L125 (1984), publisher: IOP Publishing.
 - [8] A. I. Liechtenstein, M. I. Katsnelson, and V. A. Gubanov, *Solid State Communications* **54**, 327 (1985).
 - [9] A. Szilva, M. Costa, A. Bergman, L. Szunyogh, L. Nordström, and O. Eriksson, *Phys. Rev. Lett.* **111**, 127204 (2013).
 - [10] S. Streib, R. Cardias, M. Pereiro, A. Bergman, E. Sjöqvist, C. Barreateau, A. Delin, O. Eriksson, and D. Thonig, *Phys. Rev. B* **105**, 224408 (2022), publisher: American Physical Society.
 - [11] S. Streib, A. Szilva, V. Borisov, M. Pereiro, A. Bergman, E. Sjöqvist, A. Delin, M. I. Katsnelson, O. Eriksson, and D. Thonig, *Phys. Rev. B* **103**, 224413 (2021), publisher: American Physical Society.
 - [12] R. Cardias, A. Szilva, A. Bergman, Y. Kvashnin, J. Fransson, S. Streib, A. Delin, M. I. Katsnelson, D. Thonig, A. B. Klautau, O. Eriksson, and L. Nordström, *Phys. Rev. B* **105**, 026401 (2022), publisher: American Physical Society.
 - [13] S. Brinker, M. dos Santos Dias, and S. Lounis, *Phys. Rev. Research* **2**, 033240 (2020), publisher: American Physical Society.
 - [14] R. Cardias, C. Barreateau, P. Thibaudeau, and C. C. Fu, *Phys. Rev. B* **103**, 235436 (2021), publisher: American Physical Society.
 - [15] R. Cardias, A. Bergman, A. Szilva, Y. O. Kvashnin, J. Fransson, A. B. Klautau, O. Eriksson, and L. Nordström, arXiv:2003.04680 [cond-mat] (2020), arXiv: 2003.04680.
 - [16] R. Cardias, A. Szilva, M. M. Bezerra-Neto, M. S. Ribeiro, A. Bergman, Y. O. Kvashnin, J. Fransson, A. B. Klautau, O. Eriksson, and L. Nordström, *Sci Rep* **10**, 20339 (2020), number: 1 Publisher: Nature Publishing Group.
 - [17] D. C. M. Rodrigues, A. Szilva, A. B. Klautau, A. Bergman, O. Eriksson, and C. Etz, *Phys. Rev. B* **94**, 014413 (2016).
 - [18] T. Moriya, *Phys. Rev.* **120**, 91 (1960).
 - [19] I. Dzyaloshinsky, *Journal of Physics and Chemistry of Solids* **4**, 241 (1958).
 - [20] M. dos Santos Dias, S. Brinker, A. Lászlóffy, B. Nyári, S. Blügel, L. Szunyogh, and S. Lounis, *Phys. Rev. B* **103**, L140408 (2021), publisher: American Physical Society.
 - [21] A. B. Klautau and S. Frota-Pessôa, *Phys. Rev. B* **70**, 193407 (2004).
 - [22] A. B. Klautau and S. Frota-Pessôa, *Surface Science* **579**, 27 (2005).
 - [23] A. Bergman, L. Nordström, A. Burlamaqui Klautau, S. Frota-Pessôa, and O. Eriksson, *Phys. Rev. B* **73**, 174434 (2006).

- [24] A. Bergman, L. Nordström, A. Burlamaqui Klautau, S. Frota-Pessôa, and O. Eriksson, *Phys. Rev. B* **75**, 224425 (2007), [tex.ids: bergmanMagneticStructuresSmall2007a](#).
- [25] A. Bergman, L. Nordström, A. B. Klautau, S. Frota-Pessôa, and O. Eriksson, *Surface Science* **600**, 4838 (2006).
- [26] J. Fransson, D. Thonig, P. F. Bessarab, S. Bhattacharjee, J. Hellsvik, and L. Nordström, *Phys. Rev. Materials* **1**, 074404 (2017), publisher: American Physical Society.
- [27] T. Kikuchi, T. Koretsune, R. Arita, and G. Tatara, *Phys. Rev. Lett.* **116**, 247201 (2016).
- [28] A. Crépieux and C. Lacroix, *Journal of Magnetism and Magnetic Materials* **182**, 341 (1998).
- [29] S. Brinker, M. dos Santos Dias, and S. Lounis, *New Journal of Physics* **21**, 083015 (2019).
- [30] A. T. Costa, R. B. Muniz, and D. L. Mills, *Phys. Rev. Lett.* **94**, 137203 (2005).
- [31] S. Heinze, K. von Bergmann, M. Menzel, J. Brede, A. Kubetzka, R. Wiesendanger, G. Bihlmayer, and S. Blügel, *Nature Physics* **7**, 713 (2011), [tex.ids: heinzeSpontaneousAtomicscale-Magnetic2011 number: 9 publisher: Nature Publishing Group](#).
- [32] M. Ozeri, J. Xu, G. Bauer, L. A. B. Olde Olthof, G. Kimbell, A. Wittmann, S. Yochelis, J. Fransson, J. W. A. Robinson, Y. Paltiel, and O. Millo, *The Journal of Physical Chemistry Letters* **14**, 4941 (2023), <https://doi.org/10.1021/acs.jpcclett.3c00702>.
- [33] S. Frota-Pessôa, *Phys. Rev. B* **46**, 14570 (1992).
- [34] S. Frota-Pessôa, A. B. Klautau, and S. B. Legoas, *Phys. Rev. B* **66**, 132416 (2002).
- [35] M. M. Bezerra-Neto, M. S. Ribeiro, B. Sanyal, A. Bergman, R. B. Muniz, O. Eriksson, and A. B. Klautau, *Sci Rep* **3**, 3054 (2013).
- [36] P. C. Carvalho, I. P. Miranda, A. B. Klautau, A. Bergman, and H. M. Petrilli, *Phys. Rev. Materials* **5**, 124406 (2021).
- [37] I. P. Miranda, A. B. Klautau, A. Bergman, D. Thonig, H. M. Petrilli, and O. Eriksson, *Phys. Rev. B* **103**, L220405 (2021).
- [38] R. Cardias, M. M. Bezerra-Neto, M. S. Ribeiro, A. Bergman, A. Szilva, O. Eriksson, and A. B. Klautau, *Phys. Rev. B* **93**, 014438 (2016).
- [39] A. Szilva, D. Thonig, P. F. Bessarab, Y. O. Kvashnin, D. C. M. Rodrigues, R. Cardias, M. Pereiro, L. Nordström, A. Bergman, A. B. Klautau, and O. Eriksson, *Phys. Rev. B* **96**, 144413 (2017).
- [40] M. S. Ribeiro, G. B. Corrêa, A. Bergman, L. Nordström, O. Eriksson, and A. B. Klautau, *Phys. Rev. B* **83**, 014406 (2011).
- [41] R. N. Igarashi, A. B. Klautau, R. B. Muniz, B. Sanyal, and H. M. Petrilli, *Phys. Rev. B* **85**, 014436 (2012).
- [42] Y. O. Kvashnin, R. Cardias, A. Szilva, I. Di Marco, M. I. Katsnelson, A. I. Lichtenstein, L. Nordström, A. B. Klautau, and O. Eriksson, *Phys. Rev. Lett.* **116**, 217202 (2016).
- [43] D. C. M. Rodrigues, A. B. Klautau, A. Edström, J. Ruzs, L. Nordström, M. Pereiro, B. Hjörvarsson, and O. Eriksson, *Phys. Rev. B* **97**, 224402 (2018).
- [44] O. K. Andersen, *Phys. Rev. B* **12**, 3060 (1975).
- [45] R. Haydock, *Computer Physics Communications* **20**, 11 (1980).
- [46] U. v. Barth and L. Hedin, *J. Phys. C: Solid State Phys.* **5**, 1629 (1972), publisher: IOP Publishing.
- [47] N. Beer and D. G. Pettifor, in *The Electronic Structure of Complex Systems*, NATO ASI Series, edited by P. Phariseau and W. M. Temmerman (Springer US, Boston, MA, 1984) pp. 769–777.